THE OFFICIAL MAGAZINE OF THE OCEANOGRAPHY SOCIETY

Oceanography

CITATION

Froelich, F., and S. Misra. 2014. Was the late Paleocene-early Eocene hot because Earth was flat? An ocean lithium isotope view of mountain building, continental weathering, carbon dioxide, and Earth's Cenozoic climate. *Oceanography* 27(1):36–49, http://dx.doi.org/10.5670/oceanog.2014.06.

DOI

http://dx.doi.org/10.5670/oceanog.2014.06

Was the Late Paleocene-Early Eocene Hot Because Earth Was Flat?

An Ocean Lithium Isotope View of Mountain Building, Continental Weathering, Carbon Dioxide, and Earth's Cenozoic Climate

BY FLIP FROELICH AND SAMBUDDHA MISRA

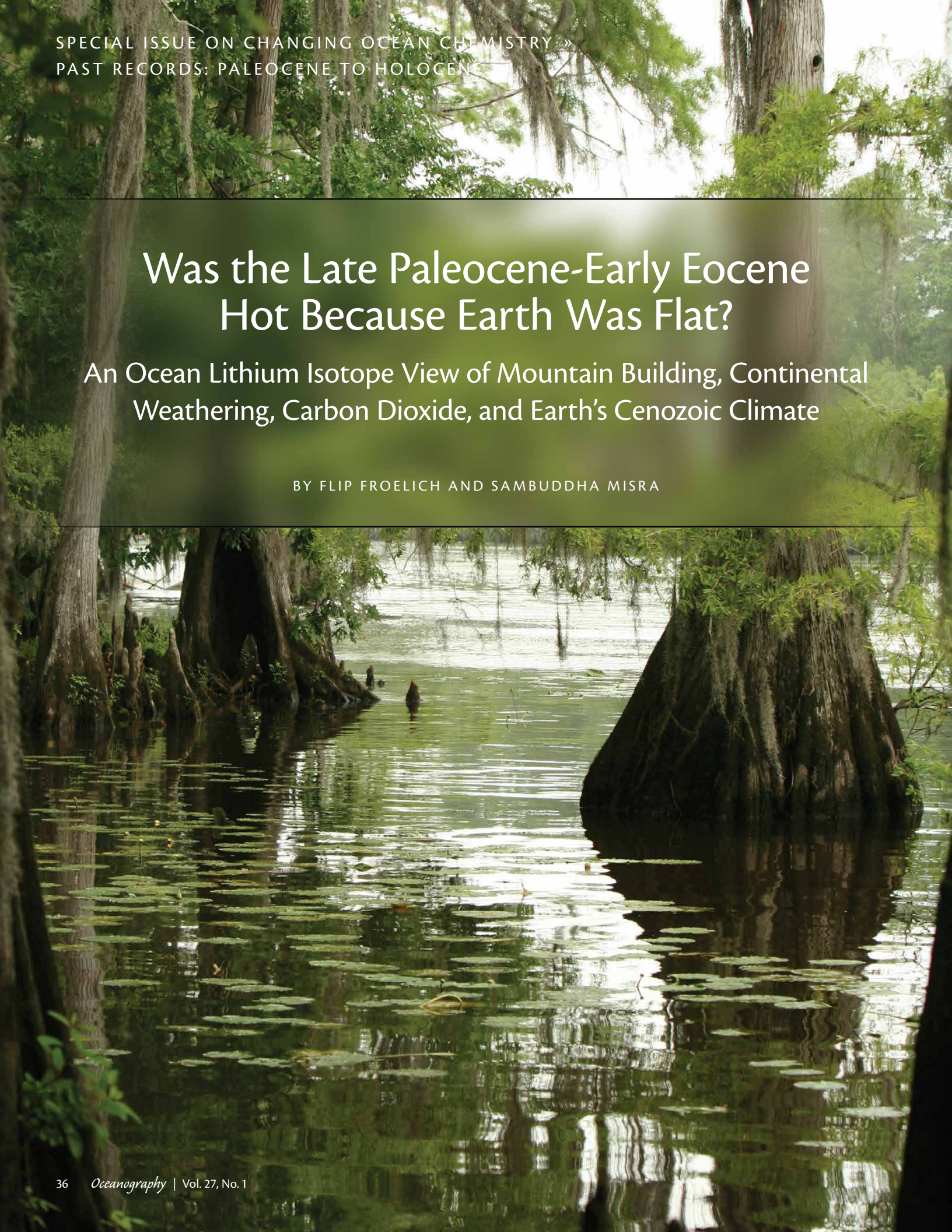

ABSTRACT. Hothouse climates in Earth's geologic past, such as the Eocene epoch, are thought to have been caused by the release of large amounts of carbon dioxide and/or methane, which had been stored as carbon in biogenic gases and organic matter in sediments, to the ocean-atmosphere system. However, to avoid runaway temperatures, there must be long-term negative feedbacks that consume CO_2 on time scales longer than the ~ 100,000 years generally ascribed to ocean uptake of CO_2 and burial of marine organic carbon. Here, we argue that continental chemical weathering of silicate rocks, the ultimate long-term (multi-million year) sink for CO_2, must have been almost dormant during the late Paleocene and early Eocene, allowing buildup of atmospheric CO_2 to levels exceeding 1,000 ppm. This reduction in the strength of the CO_2 sink was the result of minimal global tectonic uplift of silicate rocks that did not produce mountains susceptible to physical and chemical weathering, an inversion of the Uplift-Weathering Hypothesis. There is lack of terrestrial evidence for absence of uplift; however, the δ^7Li chemistry of the Paleogene ocean indicates that continental relief during this period of the Early Cenozoic was one of peneplained (flat) continents characterized by high chemical weathering intensity and slow physical and chemical weathering rates, yielding low river fluxes of suspended solids, dissolved cations, and clays delivered to the sea. Only upon re-initiation of mountain building in the Oligocene-Miocene (Himalayas, Andes, Rockies) and drifting of these continental blocks to low-latitude locations near the Inter-Tropical Convergence Zone and monsoonal climate belts did continental weathering take on modern characteristics of rivers with high suspended loads and incongruent weathering, with much of the cations released during weathering being sequestered into secondary clay minerals. The δ^7Li record of the Cenozoic ocean provides another piece of circumstantial evidence in support of the Late Cenozoic Uplift-Weathering Hypothesis.

INTRODUCTION

Earth's climate and the chemistry of its global ocean are intricately linked via (1) the chemical weathering of igneous silicate rocks on land, which consumes CO_2 and releases cations and alkalinity to the sea, and (2) the re-formation and uplift of igneous rocks during plate collision and subduction, which releases CO_2 (Urey and Korff, 1952; Holland, 1978; Walker et al., 1981; Berner et al., 1983; Raymo et al., 1988; Raymo, 1991; Raymo and Ruddiman, 1992; Ruddiman et al., 1997). This Urey-Walker-Berner rock chemistry cycle (see Box 1) is dependent on four processes: the planet's system of continental drift, seafloor spreading, and plate tectonics; mountain building by continental-continental and continental-oceanic crust collisions; subduction; and arc volcanism. The cycle is generally thought to form the basis for the long-term (multi-million year) feedbacks that have kept Earth's climate from running away to either permanent hothouse or icehouse conditions. The details of these uplift-climate linkages can be discovered by unraveling the past histories of climate change and ocean chemistry that were markedly different from today over long periods of Earth's past.

The Eocene epoch, about 56 to 34 million years ago (Ma), is one such example of an extreme climate, with very warm temperatures, up to 5°C (low latitude) and 10°C (high latitude) warmer than today (Zachos et al., 2001, 2005, 2008; Sluijs et al., 2006). Low-latitude surface ocean temperatures may have approached 40°C and bottom water temperatures were as warm as 12°C, apparently lacking high-latitude cold, dense bottom water sources. There were no high-latitude ice caps on the poles, and, as a result, sea level was almost 100 m higher than today. The continental shelves were swamped. Inland epicontinental seas were prevalent. Evolution was still recovering from the Cretaceous-Paleogene bolide impact and the Deccan Trap eruptions (KPg Boundary, 66 Ma) that killed off the dinosaurs, destroyed over 75% of all extant genera, and left the surface ocean and continental land masses with a depaupered ecological diversity incapable of producing massive amounts of organic carbon (Alvarez et al., 1980; Courtillot and Renne, 2003).

Flip Froelich *(pfroelich@comcast.net) is Chief Scientist, Froelich Education Services, Tallahassee, FL, USA.* **Sambuddha Misra** *is Postdoctoral Researcher, Department of Earth Sciences, University of Cambridge, Cambridge, UK.*

The beginning of this "Hot Eocene" was the Paleocene-Eocene Thermal Maximum (PETM, 56 Ma), a short period when atmospheric CO_2 concentrations peaked at over 1,000 ppm, almost four times that of our current pre-Anthropocene atmosphere (Figure 1; Zachos et al., 2001, 2005; Beerling and Royer, 2011). The ocean carbonate compensation depth (CCD) was about 1,500 m shallower than today at the onset of the Early Eocene Climatic Optimum (EECO, 52 Ma) (Pälike et al., 2012), reflecting high levels of seawater CO_2 and ocean acidification (Zachos et al., 2005). Most of the literature dealing with this period—the PETM, the EECO, and the periodic hyperthermals—has emphasized the supply side of the CO_2 balance (Zachos et al., 2008) to explain not only high persistent CO_2 but also sudden carbon isotope excursions (CIE) during orbitally paced hyperthermals that each seem to have lasted about 100,000 years. These CIE events have been variously interpreted as "burps" and "bleeds" releasing (1) isotopically light methane from warmed sedimentary gas hydrate reservoirs (Zeebe, 2013, and references therein), (2) thermogenic CO_2 and CH_4 from cooking of sedimentary organic carbon by magmatic intrusions into organic-rich sediments (Svensen et al., 2004), (3) CO_2 during subduction of carbon-rich upwelling sediments (Reagan et al., 2013), (4) CO_2 from burning of peatlands (Kurtz et al., 2003), and (5) CO_2 during subduction of carbonate-laden oceanic crust upon collision and closure of the low-latitude Tethys Seaway and initiation of the western Pacific subduction zones (Bouihol et al., 2013). A decrease in the burial of organic matter, not a source but rather a "missing sink" that would leave light carbon dioxide behind in the atmosphere-ocean system (e.g., Komar et al., 2013), has also been argued. Change in the ultimate carbon sink (continental weathering of silicates) is often invoked to explain high CO_2 during the Eocene, but it is generally modeled with only CO_2 and temperature feedbacks on weathering rates, neglecting the importance of uplift tectonics on erosion and weathering (West et al., 2005, 2012). Evidence of absence of uplift is lacking, yet absence of evidence of uplift is abundant, leading to the apparent illusion of no connection between mountain building and climate (Hay et al., 2002).

Many models of this epoch have been incapable of reproducing the magnitude of the Eocene excursions in $\delta^{18}O$ and $\delta^{13}C$ or the increase in CO_2 and consequent shoaling in the depth of the oceanic CCD (see below) (Sluijs et al., 2013; Komar et al., 2013, and references therein). The general long-term cooling trend from the middle Eocene to the Eocene-Oligocene boundary (Oi-1) and the initiation of Oligocene Antarctic glaciation and sea level drop (Figure 1) has been attributed to a slow drawdown of CO_2, but again, this is most recently ascribed to a reduction in the volcanic CO_2 source rather than an increase in the weathering of continental silicates (Lefebrve et al., 2013). Yet, one of the most important recorders of change in ocean chemistry related to continental delivery of cations to the ocean, strontium isotopes, clearly show a major change in the input of continental radiogenic ^{87}Sr to the ocean shortly after 40 Ma (Figure 2), coincident with the final collision of India with Southeast Asia (Bouihal et al., 2013) and weathering of the uplifted Himalayas (Raymo et al., 1988; Palmer and Edmond, 1989, 1992; Edmond, 1992).

In the following sections, we briefly describe how *rates* of chemical weathering of the continents (river fluxes of cations produced by silicate weathering destined for the ocean) and the *texture* of weathering intensity (the ratio of

BOX 1. THE GLOBAL UPLIFT-WEATHERING-CLIMATE CONNECTION*

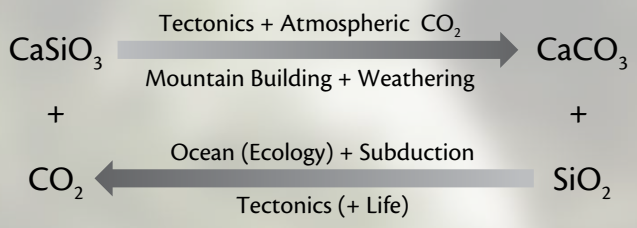

The net global reactions reflects the long-term, multi-million-year controls on atmospheric CO_2, climate, and ocean chemistry.

*Urey and Korff (1952), Holland (1978), Walker et al. (1981), Berner et al. (1983), Ruddiman et al. (1997), Raymo et al. (1988), Berner (1994), Berner and Kothvala (2001)

river-borne cations carried to the sea in dissolved form vs. that in clays) might explain the overall hothouse climate of the early Eocene. The details are contained both in the ocean chemical history of cations and in the complexities of weathering of the continents.

The basis of our argument is summarized in the feedback loops in Box 1 (Walker et al., 1981): *The long term (multi-million year) CO_2 content of the atmosphere must adjust (up or down) to the level required to achieve a quasi-steady state so that the amount of CO_2 consumed (and Ca^{2+} and Si released) during weathering of continental silicates is exactly balanced by the amount of CO_2 produced (and $CaCO_3$ + opal destroyed) during subduction.* The CO_2 content of the atmosphere-ocean system controls climate and, ultimately, global tectonics controls CO_2 concentrations. The stable isotopes of lithium (^{6}Li and ^{7}Li) are important to this theory because Li is one of the few cations that is hosted almost exclusively in silicate minerals and aluminosilicate clays and thus is directly linked to continental weathering of igneous rocks and reverse weathering in marine sediments (Aller, 2014, and references therein).

CONTINENTAL PHYSICAL AND CONGRUENT CHEMICAL WEATHERING: GLOBAL THERMOSTAT PART 1

Uplift of igneous rocks by tectonics and denudation by physical erosion provide both new mass and new surface area of reactant (silicate rocks) for chemical weathering, provided there is sufficient CO_2 to generate carbonic acid (H_2CO_3) and enough water to provide solvent. These reactions were first synthesized as acid-base neutralizations by Urey and Korff (1952), conceived as congruent dissolution reactions:

$$CaSiO_3 + 2\,CO_2 + 3\,H_2O \rightarrow Ca^{2+} + 2\,HCO_3^- + Si(OH)_4 \quad (1)$$

$CaSiO_3$ is "granite," here simplified as wollastonite. The carbon dioxide is carbonic acid in solution in rainwater, soil water, groundwater, and rivers. This CO_2 is ultimately derived from the atmosphere even though it may have been recycled through organic matter in the terrestrial regolith. The calcium silicate "granite" represents all the igneous cation-silicate minerals that contain Mg, K, Na, Sr, and Li and are presumed to weather "congruently" (i.e., homogeneously: the cations weathered and appearing in solution in rivers are the same as the cations in the igneous minerals). Two moles of CO_2 are removed from the atmosphere for every two units of alkalinity (two equivalents of cation charge) released to the sea. The dissolved calcium and other cations, bicarbonate, and dissolved silica (silicic acid; $Si(OH)_4$) are eventually washed out of soils and groundwaters and carried to the ocean

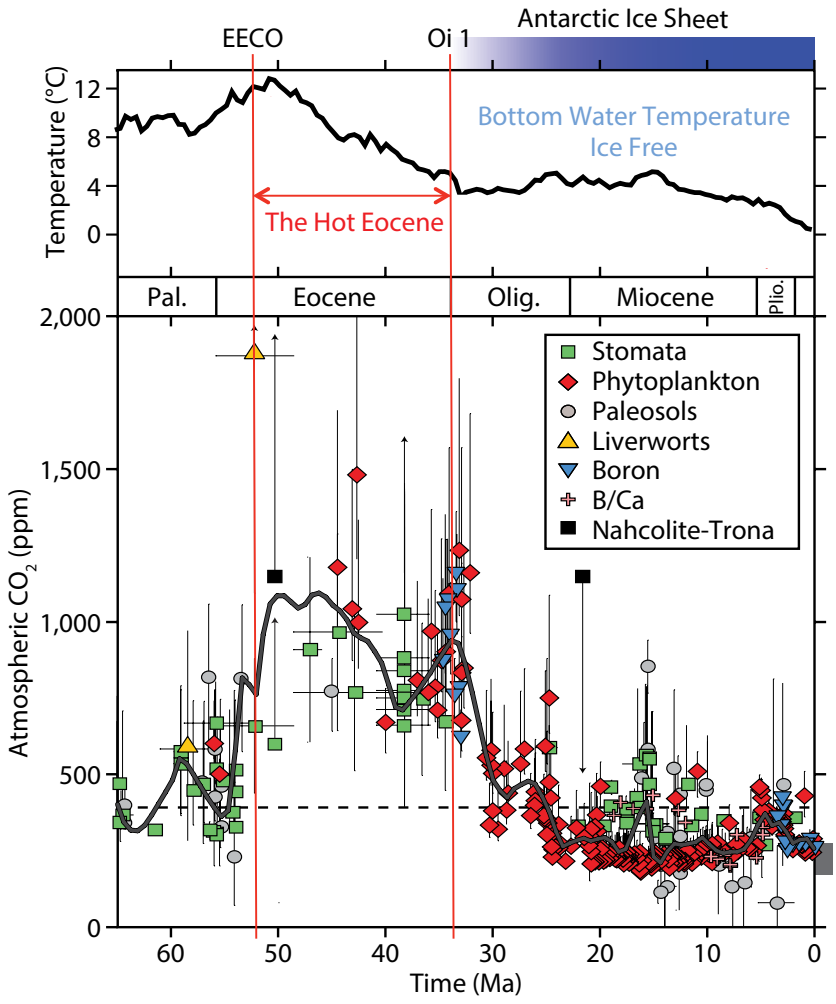

Figure 1. Multi-proxy view of Cenozoic atmospheric CO_2. Ten million years after the Cretaceous-Tertiary bolide impact at 66 million years ago (KPg, the Cretaceous-Paleogene boundary) destroyed most of the global continental and marine ecosystems, the atmospheric CO_2 rose to high values about three to four times the pre-Anthropocene (Holocene) values, perhaps to over 1,000 ppm. The Early Eocene Climatic Optimum (EECO) marks the warmest period. Oi-1 marks the first Antarctic permanent glaciation at the beginning of the Oligocene/ end of the "Hot Eocene." Ma = millions of years ago. *Modified from Figure 1 of Beerling and Royer (2011)*

in their dissolved forms by rivers and submarine groundwater discharge. Thus, mountains are destroyed, sea salt is created, and atmospheric CO_2 is consumed. Concepts and models of long-term climate modulation (Berner et al., 1983; Berner, 1994; Berner and Kothavla, 2001) generally take the dissolved cation fluxes in rivers as the rates of cations released by igneous silicate mineral reactions and set this equivalent to the CO_2 consumed from the atmosphere. There are, of course, additional physical and chemical weathering reactions on the continents (sedimentary conglomerates, limestones, dolomites, shales, evaporites), but as Walker et al. (1981) pointed out, it's the igneous silicate minerals that matter for long-term consumption of CO_2 on global tectonic time scales. We contend that uplift and erosion-denudation of igneous rocks set the long-term rates (see Chamberlin, 1899, for origin of this idea, Holland, 1978, for its modern explication, and Hay et al., 2002, and West et al., 2012, for a more complete discussion of the ideas on climate stabilization of chemical weathering rates by denudation and erosion rates).

One problem with the above reactions in CO_2 models is the assumption of congruency, that all cations released by chemical weathering end up in the dissolved load delivered to the ocean as alkalinity, that there are no solid phase products of chemical weathering. The production of secondary clay minerals carrying cations in particulate matter is generally ignored—incongruent weathering. We return to this problem below in the concept of chemical weathering intensity.

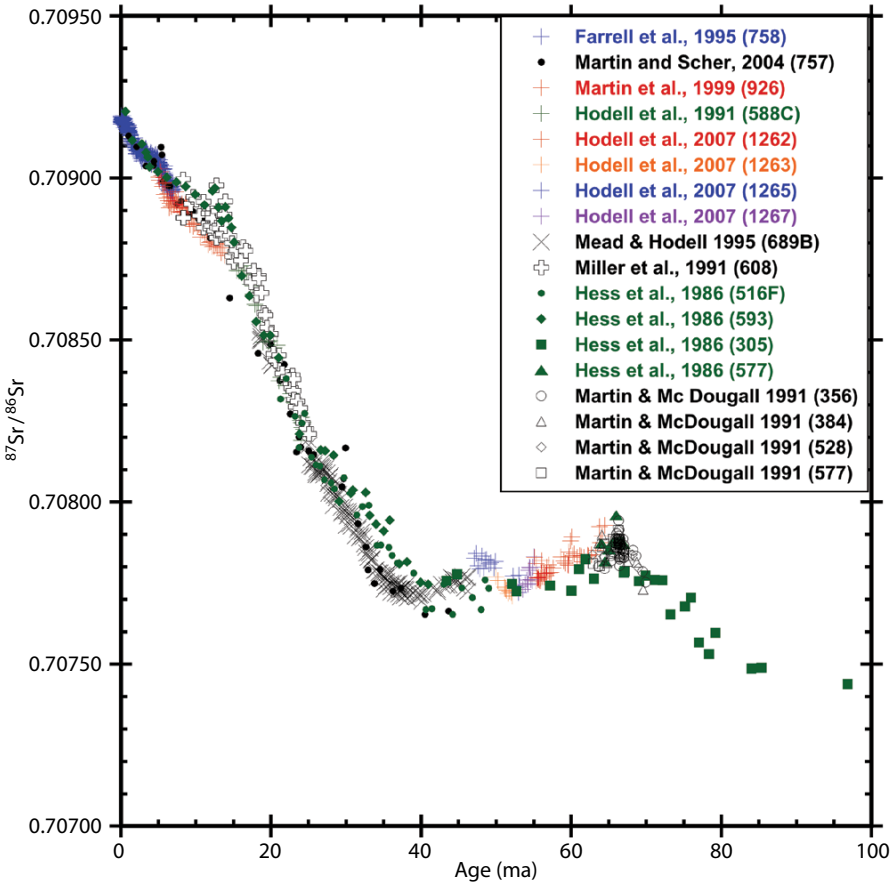

Figure 2. History of seawater strontium isotope ratios. Higher values (higher radiogenic ^{87}Sr) toward the present are generally interpreted as reflecting greater influence of continentally weathered Sr entering the ocean from about 40 Ma, driven at least in part by the collision of India with Southeast Asia and tectonic uplift and erosion of the Himalayas. Data are from: Hess et al., 1986; Martin and McDougall, 1991; Miller et al., 1991; Hodell et al., 1991, 2007; Mead and Hodell, 1995; Farrell et al., 1995; Martin et al., 1999; Martin and Scher, 2004. *Modified from Misra and Froelich (2012)*

OCEANIC CALCIFICATION AND SILICIFICATION: GLOBAL THERMOSTAT PART 2

$$Ca^{2+} + 2\,HCO_3^- \rightarrow CaCO_3 + H_2O + CO_2 \quad (2)$$

$$Si(OH)_4 \rightarrow SiO_2 + 2\,H_2O \quad (3)$$

Calcifying and silicifying plankton in the surface ocean take up dissolved calcium and silica that are delivered to the sea by rivers and use them to produce shells that are then delivered to the seabed where they accumulate as carbonate- and silica-rich sediments (limestone and opal). Note that one mole of the two moles of CO_2 taken up in reaction (1) are released by marine carbonate production in reaction (2).

PLATE TECTONICS AND SUBDUCTION: GLOBAL THERMOSTAT PART 3

$$CaCO_3 + SiO_2 \rightarrow CaSiO_3 + CO_2 \quad (4)$$

Reaction (4) reflects the transport by plate tectonics of sediment-laden oceanic crust to deep subduction zones where high heat and pressure fuse the limestone and opal to create new "granite" (wollastonite) magmas that are brought back to Earth's surface via volcanic activity, a process that releases a mole of CO_2. The ocean (reactions 2 and 3) provides the shuttle that connects the uplift and

weathering of the continents with the re-formation of continental rocks during subduction. The rates of reactions (1) and (4) compete to reach a steady state of atmospheric CO_2 concentrations. These rates are dependent on plate tectonics (uplift and subduction) and on the CO_2, temperature, and erosion feedbacks on weathering (Walker et al., 1981; Berner et al., 1983; West et al;, 2012). While these are simplified versions of complicated processes, they suffice to illustrate the long-term tectonic control of CO_2 that sets the planet's thermostat. The net global reaction (Box 1) reflects the long-term, million-year controls on atmospheric CO_2, climate, and ocean chemistry.

INCONGRUENT WEATHERING, CLAYS, AND LITHIUM ISOTOPES

Igneous minerals seldom weather congruently to deliver only dissolved cations and silica; intermediate cation-bearing clay minerals are also produced. These clays are silica deficient and alumina enriched—the secondary aluminosilicate residues in soils. They are ubiquitous, complex, generally of mixed fine phases, and virtually impossible to separate and identify from the mass of other fine phase primary minerals and oxides accumulating in soils and being transported by rivers. For example, the *incongruent* weathering of k-feldspar (orthoclase) to form a potassium mica clay (biotite) is written:

$$3/2\ KAlSi_3O_8 + CO_2 + 7\ H_2O \rightarrow \tfrac{1}{2}\ KAl_3Si_3O_{10}(OH)_2 + K^+ + 3\ Si(OH)_4 + HCO_3^- \quad (5)$$

(K-feldspar + carbon dioxide ⟶ K-mica + dissolved potassium, silica, and bicarbonate)

The potassium that ends up in the clay k-mica has been weathered from orthoclase and has consumed CO_2, and if it is delivered to the ocean intact, then it represents a potassium weathered from an igneous mineral but not delivered to the sea as alkalinity (i.e., dissolved K^+). If the potassium is weathered from the mica prior to particulate removal,

$$2\ KAl_3Si_3O_{10}(OH)_2 + 2\ CO_2 + 5\ H_2O \rightarrow 3\ Al_2Si_2O_5(OH)_4 + 2\ K^+ + 2\ HCO_3^- \quad (6)$$

(K-mica + carbon dioxide ⟶ kaolinite + dissolved potassium and bicarbonate)

The requisite CO_2 is consumed to balance the potassium released from weathering the clay. The new clay mineral produced, kaolinite, contains no cations.

$$Al_2Si_2O_5(OH)_4 + 5\ H_2O \rightarrow 2\ Al(OH)_3 + 2\ Si(OH)_4 \quad (7)$$

(kaolinite ⟶ gibbsite + dissolved silica)

Kaolinite dissolution does not consume CO_2 as there are no cations released—it is not an acid-base reaction but rather simple dissolution. It is congruent with respect to Si (all Si in kaolinite is released to solution) but incongruent with respect to Al (which ends up as gibbsite). Although experimental data are lacking that might demonstrate this reaction, octahedral Mg (and Li) in kaolinite are presumably released to solution during its dissolution.

RIVERS AND LITHIUM ISOTOPES

The importance of these clay mineral reactions is that Mg commonly substitutes for Al in the structural octahedral sites of many secondary clays formed by weathering—kaolinites, smectites, and illites. Lithium, because it has the same ionic size, easily substitutes for octahedral Mg (Decarreau et al., 2012), especially in mixed-layer smectites that dominate secondary mixed-layer clays. Li produced by the weathering of igneous minerals then has two fates: (1) it remains in the dissolved phase of rivers and groundwaters and is delivered to the sea, or (2) it is incorporated into secondary aluminosilicate clays. This clay-Li is isotopically very light compared to the Li in mother solutions (Huh et al., 1998, 2001; Kisakurek et al., 2005; Vigier et al., 2006, 2008, 2009; Pogge von Standmann et al., 2006, 2008; Millot et al., 2010; Wimpenny et al., 2010). In addition, virtually all (95%) of the Li cycled on Earth's surface resides in silicates and aluminosilicates (Stoffyn-Egly and Mackenzie, 1984; Misra and Froelich, 2012). There is little lithium in limestones, dolomites, biosiliceous deposits, or evaporites. The trace Li_2CO_3 in evaporites (precipitated from Li in seawater) is easily identified in rivers draining these deposits because of the correlations with chloride and sulfate. Like the evaporite- and limestone-derived Na, Ca, Mg, Cl, and SO_4 in rivers, the Li flux in rivers due to recycled marine evaporites and carbonates is easily subtracted from the fluvial Li burden in order to obtain the silicate-weathered component only.

Thus, the isotopic offset between source (Li in igneous minerals) and product (Li in clays) results in the dissolved Li in rivers and groundwaters being isotopically very heavy (Huh et al., 2001). The δ^7Li values of igneous minerals in granites and basalts do not vary greatly (values generally lie between 0‰ and + 4‰). The average global river dissolved δ^7Li values are about 21‰ heavier than their rock-Li sources (Figure 3). Today, this reflects a global partitioning between dissolved-Li and clay-Li of about 1:4. In other words, the difference between the heavy dissolved river Li and the source rocks requires about 80% of the Li derived

from igneous rock dissolution to end up in clays regardless of whether these clays remain behind in soils or are transported undissolved to the sea. The systematics of river-dissolved δ^7Li are complicated by enormous heterogeneity because the complementary solid phase secondary clays cannot be separated from the detrital fine phases in rivers, and because the distribution and transport of Li in secondary clays (particulates) and dissolved Li (solution) are discontinuous in both space and time. As a result, analyses of river grab samples with suspended material containing secondary clays and dissolved Li do not reflect in situ weathering processes except in the broadest, whole drainage basin, sense.

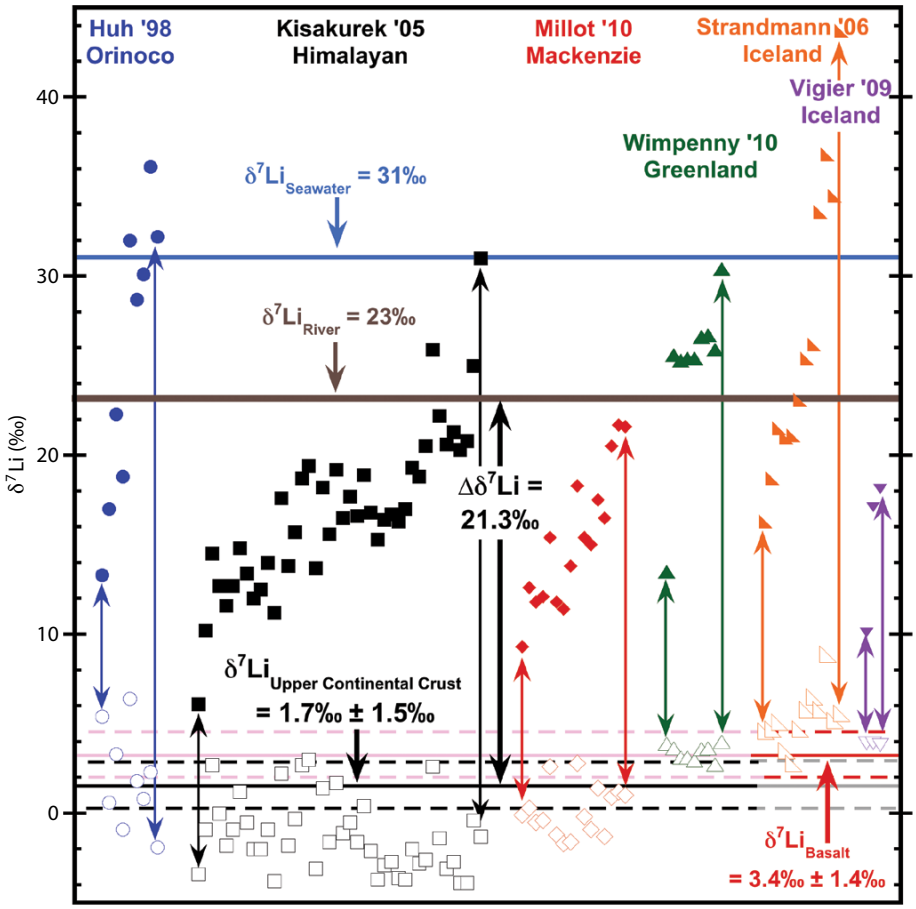

Figure 3. δ^7Li compositions of suspended and dissolved river loads in all rivers that have been simultaneously analyzed for both. The paired data from each of these six rivers were first arranged in order of increasing difference between dissolved and particulate δ^7Li without regard to concentrations, distance downstream, or dissolved/particulate ratios. Each pair of data for each river was then plotted with increasing pair difference from left to right. Solid colored symbols are dissolved δ^7Li. Open symbols of the same shape and color are the paired suspended particulate δ^7Li. The right-most data pair and the left-most data pair of each river set are connected by a vertical straight barbed color line denoting the least (left) and the greatest (right) differences for each pair. The vertical connection lines for the data pairs in between have been omitted for clarity. The δ^7Li values for seawater (31‰) and average dissolved river waters (23‰) are given as horizontal solid blue and mauve lines. The average values of the upper continental crust (UCC; 1.7‰) and average basalts (3.4‰) are given as horizontal solid black and red lines bounded by their ranges (dashed lines). The average fractionation between the UCC and dissolved rivers (about 21.3‰) is given as the heavy vertical double-ended arrow in the middle of the figure. Data sources are given in the appendices of Misra and Froelich (2012). The blue circles are results from Orinoco basin (Huh et al., 2001), the black squares from Himalayan rivers (Kisakurek et al., 2005), red diamonds from Mackenzie River (Millot et al., 2010), green triangles from Greenland rivers (Wimpenny et al., 2010), orange triangles from Icelandic rivers (Pogge von Strandmann et al., 2006), and purple triangles from Icelandic rivers (Vigier et al., 2009). The studies on Icelandic rivers by Pogge von Strandmann et al. (2006) and Vigier et al. (2009) drain basaltic terrains. The Himalayan rivers, Orinoco basin, and Mackenzie River studies cover a wide range of terrains dominated by granites, shales, carbonates, and evaporites.

For example, in Figure 3, the δ^7Li differences between dissolved and suspended Li in rivers are queued up in rank order of increasing δ^7Li offsets from left to right (see Figure 3 legend for details of this plotting protocol). If rivers were laboratory bottle weathering experiments, we would expect a simple relationship—as dissolved-Li δ^7Li increases (from left to right across the plot), the corresponding clay-Li (particulate δ^7Li) should decrease from left to right. This latter effect for the particulates is barely discernible in the plot. The reasons are threefold. First, the particulates in the fine phase include random mixtures of secondary aluminosilicate and primary igneous minerals—the latter dilutes the isotopic signal we would wish to identify in the clay minerals. Second, the aluminosilicate clay δ^7Li that represents the dissolved δ^7Li was formed somewhere and sometime else than where the river sample was grabbed. Third, mixing of river waters and particulates downstream from the rock weathering locations (soils? groundwaters?) precludes identifying the primary isotopic sources for either phase.

Nevertheless, Figure 3 does contain important information. The data with the highest offsets (the right side of each river grouping with the heaviest δ^7Li) come from portions of the drainages with the highest relief and igneous silicate lithologies. The data with the lowest

offsets and lowest dissolved δ^7Li typically arise from more intensely weathered low-relief regions of each drainage basin. We interpret this as the dissolved-Li δ^7Li signature of weathering intensity in today's world (see Box 2). Low weathering intensity regimes (weathering limited) with steep relief, fast uplift, and incongruent weathering generally tend to display heavy dissolved δ^7Li with clays carrying light δ^7Li in their octahedral sites (e.g., cation analogs to reactions 5 and 6). The ratio of clay-Li to dissolved-Li is high—most of the weathered cation-Li ends up in secondary clays. High weathering intensity (transport limited) rivers with flat relief (peneplains) tend to display light δ^7Li and little secondary octahedral clays. Cation weathering is congruent. Clays carrying light δ^7Li are dissolving (reaction 7), not forming. The ratio of clay-Li to dissolved-Li is low and all of the weathered cations end up in the dissolved load.

Although high weathering intensity terrains are poorly represented today in the global river δ^7Li data set (and on the present-day globe in general), we argue below that the intensely weathered low latitudes of our Eocene planet were dominated by these flat-land, water-saturated drainages. Eocene global chemical weathering texture was much more congruent and highly intense than during the Late Cenozoic and delivered a very different δ^7Li_{Rivers} to the sea that dramatically affected the δ^7Li_{SW} of the ocean (Figure 4).

THE GLOBAL LITHIUM ISOTOPE CYCLE—TODAY

Today, global rivers contribute about 10×10^9 moles per year of very heavy dissolved Li to the sea (δ^7Li_{Rivers} = +23‰), much heavier than average upper continental crustal granites (δ^7Li_{UCC} = +1.7‰) (Figure 5a). Hydrothermal Li fluxes via seawater recirculating through the global mid-ocean ridge system contribute another 13×10^9 moles per year (δ^7Li_{HT} = +8.3‰), slightly heavier than basalts ($\delta^7Li_{Basalts}$ = +3.7‰). Both input fluxes are similar in magnitude and both of the dissolved fluxes are heavier than their source rock, reflecting removal of light ^{6}Li into authigenic clays (Misra and Froelich, 2012). Thus, weathering of continental and oceanic crusts today provides a dissolved Li flux to the sea that is much heavier than all rock sources (flux-weighted average δ^7Li_{Input} = +15‰). Note that these heavy inputs cannot explain the even heavier value of dissolved lithium in seawater (δ^7Li_{SW} = +31‰) (Figure 3). These isotopic offsets are enormous, the result of mass-dependent fractionation due to the large relative difference in ^{6}Li and ^{7}Li masses (16%). The secondary mineral clay-Li fraction carried down rivers to the

BOX 2. CONCEPTUAL SYNTHESIS OF END-MEMBER CONTINENTAL WEATHERING INTENSITY OF SILICATE ROCKS*

Low Weathering Intensity (weathering limited)

- Steep relief (steep grinding rivers, tectonics, uplift, mountains)
- Rapid physical weathering (high suspended solids in rivers)
- Incongruent weathering ($[Cations]_{clays}/[Cations]_{dissolved}$ is high)
- Characteristic (today) of Himalayas, Andes (monsoons, orographic rain)
- Most of "weathered" lithium delivered to the sea is in 2° clays – $[Li]_{clay}$
- Global average river lithium ratio today is 4 : 1 :: $[Li]_{clay}$: $[Li+]_{dissolved}$

High Weathering Intensity (transport limited; "supply"-limited of West et al., 2012)

- Peneplained continents (flat, sluggish rivers; no mountains in the rain belts)
- Low physical weathering (low suspended solids in rivers; very thick soils)
- Intense and congruent chemical weathering (little secondary clay formation; rock dissolution slow but homogeneous; residual alumina (gibbsite) and laterite (FeOx soils); $[Cations]_{clays}/[Cations]_{dissolved}$ is low)
- Characteristic (today) of shields in hot, wet, humid tropics (equatorial rain Inter-Tropical Convergence Zone [ITCZ] and Orinoco basin "Right Bank Guyana Shield" Rio Negro; very few examples)
- Most of "weathered" lithium delivered to sea is dissolved – $[Li]_{dissolved}$
- Global average river ratio at 60 Ma was about 1 : 4 :: [Li]clay : $[Li+]_{dissolved}$

Weathering intensity says nothing about river fluxes, which are dependent on orography (uplift) and ITCZ/monsoon runoff and rainfall. What matters is where the uplift and tectonics occur with respect to rainfall—the tropics.

** from Stallard and Edmond, 1981, 1983, 1987, and references therein*

sea (presumably without dissolution), or left behind temporarily on the continents in weathered horizons of soils, is isotopically light. The clay-Li portion delivered to the seabed is mixed with other solid components (products of physical weathering) carrying near-crustal isotope values (δ^7Li_{UCC} = +1.7‰) that swamp the light clay-Li isotope signal in sediments.

These inputs to the sea must be balanced on time scales of the Li residence time in the sea (~ 1 million years). Because Li is greatly enriched in secondary clays, and this enrichment carries light ^6Li, most studies of the lithium isotope cycle have concluded that marine removal must occur via "reverse weathering" in the ocean (Mackenzie and Garrels, 1966; Aller, 2014)—the burial of Li via the re-formation of authigenic aluminosilicate clays on and in the seabed from diagenetic alteration of silica, continental clays, and detrital silicate debris (Al) and cations (especially Mg and Li) (Sayles, 1979, 1981; Mackin, 1986; Mackin and Aller, 1989; Michalopoulos and Aller, 1995, 2004; Michalopoulos et al., 2000; Aller, 2014). This removal must balance the inputs. Misra and Froelich (2012) lumped the two "known" sinks of reverse weathering into one sink: marine authigenic aluminosilicate clays (MAAC – the formation of authigenic clays in marine sediments) and altered oceanic crust (AOC – the "weathering" alteration of oceanic basalts by seawater circulation through the "low temperature" crust off axis). In both cases, the source of Li entering the MAAC and AOC diagenetic pathways is from seawater. These two processes are known to enrich light ^6Li in authigenic aluminosilicates (Chan et al., 1992, 2006; Chan and Kastner, 2000). The steady-state balance requires a net removal of about 23 × 10^9 moles per year at the δ^7Li_{Input} value of +15‰ (Figure 5a; note that we ignore the small subduction reflux in Misra and Froelich [2012] for simplicity because it has little effect on the overall long-term balance and is very poorly understood). This removal (δ^7Li_{Output} = +15‰) is 16‰ lighter than the seawater Li source (δ^7Li_{SW} = +31‰). This 16‰ offset between seawater-Li and the diagenetic-Li sink pushes seawater δ^7Li_{SW} to isotopically heavy values. Thus, about half of the present-day seawater δ^7Li_{SW} offset from rocks (+31‰) is due to heavy inputs to the ocean from crustal sources (+15‰), and about half is due to light

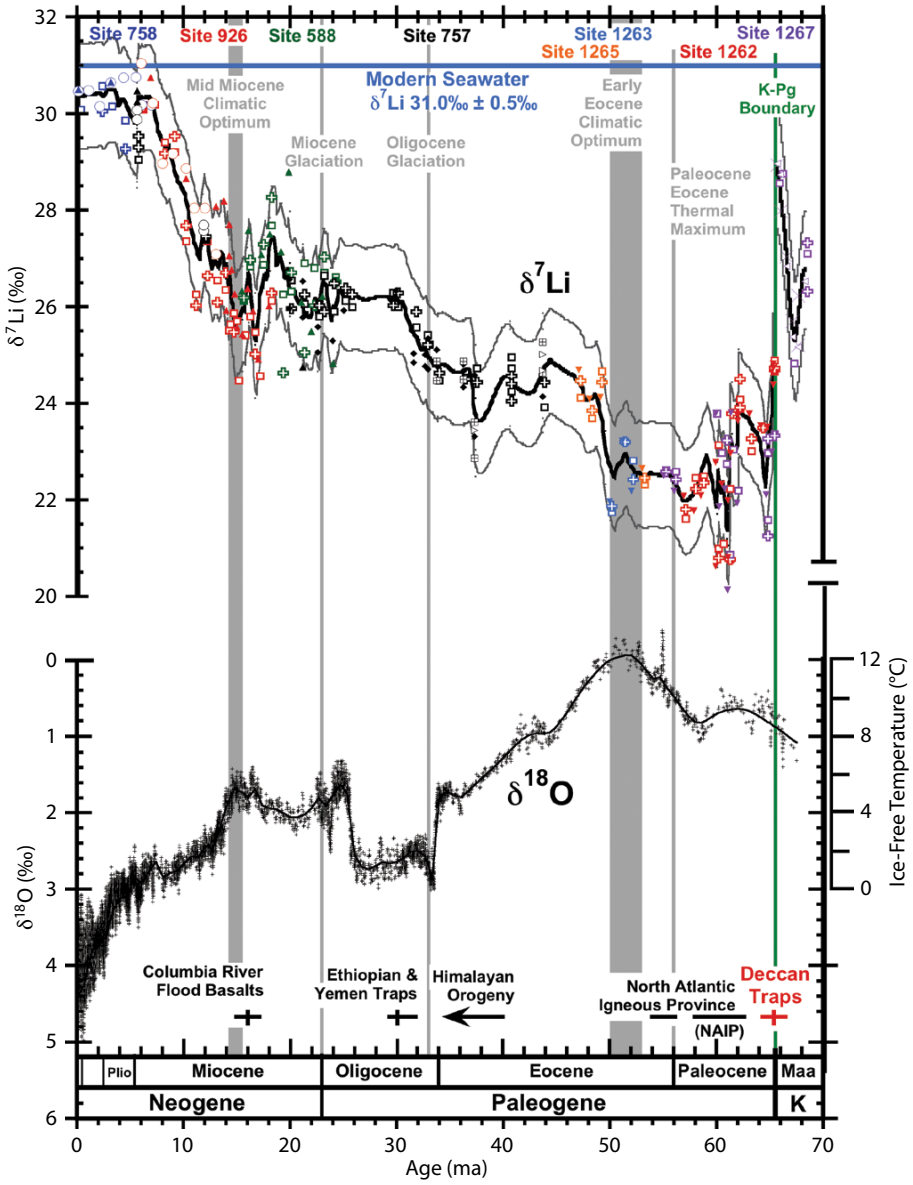

Figure 4. Lithium and oxygen isotope histories of Cenozoic seawater (from Zachos et al., 2001, 2008; Misra and Froelich, 2012, Supplementary Online Material Figure S11). The age models were not rescaled to modern chronologies so the light $\delta^{18}O$ spike at the Paleocene-Eocene Thermal Maximum (PETM) appears to be too young (it should be on the P/E boundary). The lithium isotope data are from both individual foram species and from bulk foram samples that have both been super-cleaned (see Misra and Froelich, 2012, for details of the symbols, the cleaning, and the chronologies).

outputs from the ocean into reverse weathering sinks (–16‰). Changes in input fluxes (weathering of rocks) or output fluxes (formation marine authigenic clays) or shifts in their isotopic values will force the seawater δ^7Li_{SW} to change. Such δ^7Li_{SW} changes provide clues to changes in the weathering and reverse weathering dynamics of the planet and its ocean.

THE CENOZOIC HISTORY OF SEAWATER LITHIUM ISOTOPES

Lithium incorporated into well-dated, cleaned foraminifera in marine sediments indicates that δ^7Li_{SW} has not been constant through the Cenozoic (Hathorne and James, 2006; Misra and Froelich, 2012; Figure 4). Both of these records document a rapid rise of about 4‰ from about 19 Ma until 6 Ma (middle Miocene), after which values plateaued at today's value. Misra and Froelich's (2012) record back to 68 Ma shows Late Cretaceous values that are reminiscent of this 14–6 Ma rise with a drastic 5‰ drop at the 66 Ma KPg boundary at the end of the Cretaceous. The reasons for this KPg drop are not understood, but may be related to some dramatic and fast continental or oceanic reset of weathering or reverse weathering processes that are not discussed here. Within 6 Ma after the KPg boundary, δ^7Li_{SW} values decline to a Cenozoic low of about 22‰ in the late Paleocene and early Eocene (Figure 4). We argue that this post-KPg decrease was due at least

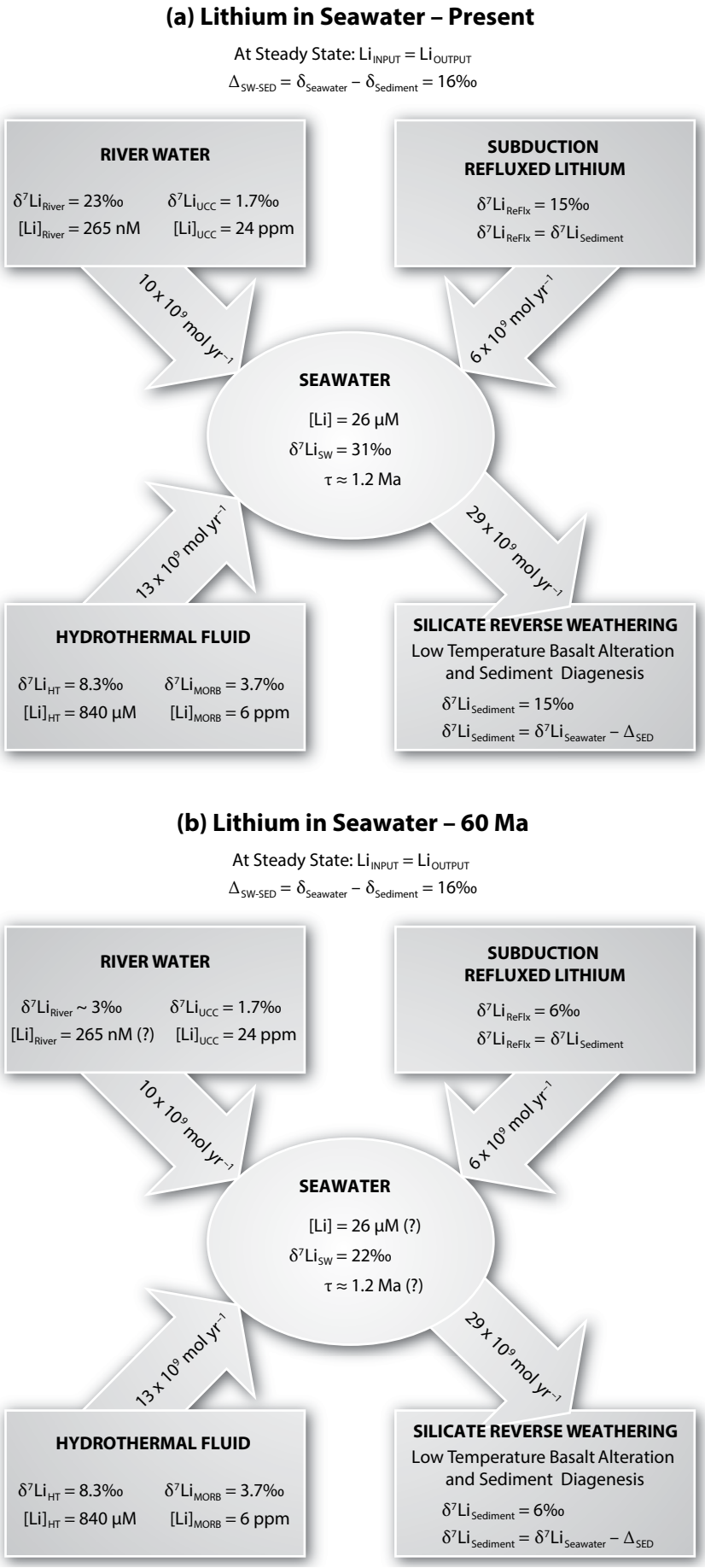

Figure 5. (a) Present-day and (b) late Paleocene (60 Ma) depictions of steady-state lithium and lithium isotope fluxes to and from the ocean (modified after Misra and Froelich, 2012). Note that Li and West (2014) partition the reverse weathering sink into two components, marine authigenic aluminosilicate and altered oceanic crust, with different fractionation factors. See text for their alternative explanation of the Cenozoic rise in seawater δ^7Li.

in part to a slow (5–10 Ma) Paleocene disappearance of high-relief terrains. The low value at 60 Ma is about 9‰ below today's seawater and reflects large changes in Li input or outputs, or both, compared to today. After the EECO at 52 Ma, δ^7Li_{SW} began rising in sporadic pulses. One upward shift in δ^7Li_{SW} at 51 Ma occurred after India (carrying the Deccan Traps) drifted northward across the equatorial Inter-Tropical Convergence Zone (ITCZ; Kent and Muttoni, 2008) and initiation of the collision of India with Southeast Asia. A second, at 40 Ma, occurred near the final closure of this suture and initiation of uplift of the Himalayas (Raymo and Ruddiman, 1992; Ruddiman et al., 1997; Bouihol et al., 2013). The rise of the Andes and the Rockies after about 20 Ma and 15 Ma coincides with the final upticks in the δ^7Li_{SW} record.

Coincidence does not prove causality, but the implications of the seawater δ^7Li record are that (1) if the seawater δ^7Li_{SW} change is being driven by changes in continental weathering, and (2) if the Li isotope fractionation exhibited by clays is a general feature of Li transfer into authigenic aluminosilicates, then the Cenozoic δ^7Li_{SW} record is most easily interpreted as one of increasing relief and uplift, decreasing continental weathering intensity leading to more incongruent weathering, more cations in clays, and faster denudation in the Late Cenozoic. The early Eocene must have been largely deficient in these features.

THE GLOBAL LITHIUM ISOTOPE CYCLE— 60 MILLION YEARS AGO

A possible lithium isotope balance for the Paleocene/Eocene boundary ocean at 60 Ma is one in which the entire δ^7Li_{SW} change (9‰) is delegated to the continental weathering source—all else remaining constant, including invariant hydrothermal fluxes (Rowley, 2002) and lithium isotope fractionation factors (Misra and Froelich, 2012; Figure 5b). In this simple end-member scenario, which is unlikely to be the whole answer, continental rivers must exhibit almost congruent weathering with very high weathering intensity (δ^7Li_{Rivers} = +3‰), peneplained low relief continents in the tropical rainfall belts, low physical weathering with low suspended solids in rivers, and low dissolved-Li to clay-Li ratios (Box 2). This is consistent with age-, subduction-, and hiatus-loss corrected seafloor drill core records for Cenozoic Deep-Sea Drilling Project and Ocean Drilling Program sites showing that terrestrial sediment accumulation rates on the seafloor, which must reflect global denudation rates of detrital material to the seabed, increased dramatically in the Neogene (Peizhen et al., 2001; Hay et al., 2002; Molnar, 2004; Herman et al., 2013, and references therein). In contrast, the continental delivery of material to the Paleogene sea consisted mostly of dissolved chemicals, with minimal solid detritus. The Eocene seafloor record shows large deposits of cherts (biogenic opal), phosphorites, organics, and a shallow CCD with shallow-water (reefal) carbonates (Brewster, 1980; Pälike et al., 2012). Paleogene ocean Mg/Ca ratios were a factor of three to five times lower than today (Holland, 1978; Coggon et al., 2010; Rausch et al., 2013), suggesting that the continental delivery of seawater ions (Mg, Li) via weathering and their loss to the seafloor via reverse weathering were both reduced compared to today.

Li and West (2014) make a good case for Cenozoic changes in both continental weathering and in seafloor reverse weathering to explain the Cenozoic δ^7Li_{SW} records. In their model, they partition the reverse weathering sink into explicit and separate AOC and MAAC components and apply different temperature-dependent fractionation factors to each. For the MAAC sediment component, they adopt a lithium isotope fractionation offset from seawater of $\Delta_{SW\text{-}MAAC}$ = 20‰. For the AOC component, they adopt a Li-fractionation factor based on expected warm temperatures in oceanic crust undergoing alteration of $\Delta_{SW\text{-}AOC}$ = 13‰ (about 80°C; Chan et al., 2002). This 7‰ spread in the two components of $\Delta_{Rev\text{-}Wx}$ is in contrast to the single value for reverse weathering of 16‰ adopted by Misra and Froelich (2012). Then, they scale the continental Li flux to the Cenozoic CO_2/ocean dissolved inorganic carbon model of Li and Elderfield (2013) to estimate continental weathering fluxes—these increased fluxes explain about half the oceanic δ^7Li_{SW} rise of the past 60 Ma. They can balance the other half of the ocean rise in δ^7Li_{Rivers} by scaling an increase in the MAAC reverse weathering sink to increased continental weathered detritus (Al-source) delivered to the seafloor by the increased physical denudation of the continents derived from their weathering model. They find that to explain the full change in Cenozoic seawater δ^7Li_{SW} (9‰), their model δ^7Li_{Rivers} must increase from a low of about 9.6‰ +/– 3.0‰ at 60 Ma to the present-day value of 23.5‰, an increase of about 13‰ +/– 3‰. This is about half of the change in continental weathering explored by the end-member scenario of Misra and Froelich (2012) and avoids their extremely high weathering intensity at the Paleocene/Eocene boundary. More importantly, the Li and West (2014) result would about double weathering fluxes of continental dissolved lithium

fluxes (rivers) and increase the burial flux of MAAC on the seafloor by a factor of about 3.0. These changes reflect dramatic shifts in continental weathering and the delivery of detritus and cation dissolved-Li and clay-Li to the sea over the Cenozoic. We estimate from their model that the clay-Li to dissolved-Li ratio of continental rivers increased from 1:2 at 60 Ma ago to 3:1 at present (cf. Box 2), so that if the dissolved Li-flux increased by a factor of 2, the clay-Li delivery flux to the ocean rose by a factor of 12, and the total lithium weathered from igneous rocks on the continents rose about a factor of 15.

Clearly, if these changes in continental lithium fluxes scale in any manner to other cations weathered from the continents (especially Mg), then the consumption of CO_2 by silicate weathering and the release of cations to the sea increased dramatically over the Cenozoic, implying the absence of these factors driven by uplift and high relief in the early Eocene.

CONCLUDING REMARKS

The early Cenozoic climatic optimum was a result of increased supply of carbon dioxide to the ocean-atmosphere system as well as diminished removal of carbon dioxide from the atmosphere through weathering of silicate rocks. The scarcity of newly uplifted, fresh, weatherable rocks in the hothouse climate led to a slowdown of the negative feedback mechanism of the Urey-Walker-Berner cycle and promoted a *temporary runaway* increase in the CO_2 concentrations of the ocean-atmosphere system on the post-KPg Earth. The absence of evidence from seawater $^{87/86}Sr$ and δ^7Li records to support increased continental weathering rates in this high-CO_2 hothouse world indicates that the limiting ingredient was igneous silicates undergoing weathering. While this Paleocene-Eocene Earth was probably not flat, evidence from the ocean suggests that despite global high temperatures, high CO_2, and high rainfall in the tropics (all of which should accelerate silicate weathering and promote removal of CO_2), the physical and chemical weathering rates of the continents were subdued because of low uplift rates. CO_2 consumption and cation release by silicate weathering was lower than today. Fluxes of dissolved cations, continental detritus, and secondary detrital clays to the seabed were also significantly lower than today. Formation of authigenic aluminosilicate clays via reverse weathering in marine sediments was limited. This "absence of a CO_2 sink" hypothesis might help explain how the hot Eocene climate persisted for tens of millions of years.

ACKNOWLEDGEMENTS

We thank Josh West, Mark Torres, and an anonymous reviewer for useful comments.

REFERENCES

Aller, R.C. 2014. Sedimentary diagenesis, depositional environments, and benthic fluxes. Pp. 293–334 in *Reference Module in Earth Systems and Environmental Sciences*, *Treatise on Geochemistry, 2nd ed., The Oceans and Marine Geochemistry,* vol. 8. Elsevier, http://dx.doi.org/10.1016/B978-0-08-095975-7.00611-2.

Alvarez, L.W., W. Alvarez, F. Asaro, and H.V. Michel. 1980. Extraterrestrial cause for the Cretaceous-Tertiary Extinction. *Science* 208:1,095–1,108, http://dx.doi.org/10.1126/science.208.4448.1095.

Beerling, D.J., and D.L. Royer. 2011. Convergent Cenozoic CO_2 history. *Nature Geoscience* 4:418–420, http://dx.doi.org/10.1038/ngeo1186.

Berner, R.A. 1994. GEOCARB II: A revised model of atmospheric CO_2 over Phanerozoic time. *American Journal of Science* 294:56–91, http://dx.doi.org/10.2475/ajs.294.1.56.

Berner, R.A., and A. Kothavla. 2001. GEOCARB III: A revised model of atmospheric CO_2 over Phanerozoic time. *American Journal of Science* 301:182–204, http://dx.doi.org/10.2475/ajs.301.2.182.

Berner, R.A., A.C. Lasaga, and R.M. Garrels. 1983. The carbonate-silicate geochemical cycle and its effect on atmospheric carbon dioxide over the past 100 million years. *American Journal of Science* 283:641–683, http://dx.doi.org/10.2475/ajs.283.7.641.

Bouihol, P., O. Jagoutz, J.M. Hanchar, and F.O. Dudas. 2013. Dating the India-Eurasia collision through arc magmatic records. *Earth and Planetary Science Letters* 366:163–175, http://dx.doi.org/10.1016/j.epsl.2013.01.023.

Brewster, N.A. 1980. Cenozoic biogenic silica sedimentation in the Antarctic Ocean. *Geological Society of America Bulletin* 6:337–347, http://dx.doi.org/10.1130/0016-7606(1980)91<337:CBSSIT>2.0.CO;2.

Chamberlin, T.C. 1899. An attempt to frame a working hypothesis for the cause of glacial periods on an atmospheric basis. *Journal of Geology* 7:545–584, http://dx.doi.org/10.1086/608449.

Chan, L.H., J.C. Alt, and D.A.H. Teagle. 2002. Lithium and lithium isotope profiles through the upper oceanic crust: A study of seawater-basalt exchange at ODP Sites 504B and 869A. *Earth and Planetary Science Letters* 201:187–201, http://dx.doi.org/10.1016/S0012-821X(02)00707-0.

Chan, L.H., J.M. Edmond, G. Thompson, and K. Gillis. 1992. Lithium isotopic composition of submarine basalts: Implications for the lithium cycle in the oceans. *Earth and Planetary Science Letters* 108:151–160, http://dx.doi.org/10.1016/0012-821X(92)90067-6.

Chan, L.H., and M. Kastner. 2000. Lithium isotopic composition of pore fluids and sediments in the Costa Rica subduction zone: Implications for fluid processes and sediment contribution to the arc volcanoes. *Earth and Planetary Science Letters* 183:275–290, http://dx.doi.org/10.1016/S0012-821X(00)00275-2.

Chan, L.H., W.P. Leeman, and T. Plank. 2006. Lithium isotopic composition of marine sediments. *Geochemistry, Geophysics, Geosystems* 7, Q06005, http://dx.doi.org/10.1029/2005GC001202.

Coggon, R.M., D.A.H. Teagle, C.E. Smith-Duque, J.C. Alt, and M.J. Cooper. 2010. Reconstructing past seawater Mg/Ca and Sr/Ca from mid-ocean ridge flank calcium carbonate veins. *Science* 327:1,114–1,117, http://dx.doi.org/10.1126/science.1182252.

Courtillot, V.E., and P.R. Renne. 2003. On the ages of flood basalt events. *Comptes Rendus Geoscience* 335:113–140, http://dx.doi.org/10.1016/S1631-0713(03)00006-3.

Decarreau, A., N. Vigier, H. Palkova, S. Petit, P. Vieillard, and C. Fontaine. 2012. Partitioning of lithium between smectite and solution: An experimental approach. *Geochimica Cosmochimica Acta* 85:314–325, http://dx.doi.org/10.1016/j.gca.2012.02.018.

Edmond, J.M. 1992. Himalayan tectonics, weathering processes, and the strontium isotope record in marine limestones. *Science* 258:1,594–1,597, http://dx.doi.org/10.1126/science.258.5088.1594.

Farrell, J.W., S.C. Clemens, and L.P. Gromet. 1995. Improved chronostratigraphic reference curve of late Neogene seawater $^{87}Sr/^{86}Sr$. *Geology* 23:403–406, http://dx.doi.org/10.1130/0091-7613(1995)023<0403:ICRCOL>2.3.CO;2.

Hathorne, E.C., and R.H. James. 2006. Temporal record of lithium in seawater: A tracer for silicate weathering? *Earth and Planetary Science Letters* 246:393–406, http://dx.doi.org/10.1016/j.epsl.2006.04.020.

Hay, W.W., E. Soeding, R.M. DeConto, and C.N. Wold. 2002. The Late Cenozoic uplift – climate change paradox. *International Journal of Earth Sciences* 91:746–774, http://dx.doi.org/10.1007/s00531-002-0263-1.

Herman, F., D. Seward, P.G. Valla, A. Carter, B. Kohn, S.D. Willett, and T.A. Ehlers. 2013. Worldwide acceleration of mountain erosion under a cooler climate. *Nature* 19:423–426, http://dx.doi.org/10.1038/nature12877.

Hess, J., M.L. Bender, and J.G. Schilling. 1986. Evolution of the ratio of strontium-87 to strontium-86 in seawater from Cretaceous to present. *Science* 231:979–984, http://dx.doi.org/10.1126/science.231.4741.979.

Hodell, D.A., G.D. Kamenov, E.C. Hathorne, J.C. Zachos, U. Röhl, and T. Westerhold. 2007. Variations in the strontium isotope composition of seawater during the Paleocene and early Eocene from ODP Leg 208 (Walvis Ridge). *Geochemistry, Geophysics, Geosystems* 8, Q09001, http://dx.doi.org/10.1029/2007GC001607.

Hodell, D.A., P.A. Mueller, and J.R. Garrido. 1991. Variations in the strontium isotopic composition of seawater during the Neogene. *Geology* 19:24–30, http://dx.doi.org/10.1130/0091-7613(1991)019<0024:VITSIC>2.3.CO;2.

Holland, H.D. 1978. *The Chemistry of the Atmosphere and Ocean.* Wiley, New York, 369 pp.

Huh, Y., L.H. Chan, and J.M. Edmond. 2001. Lithium isotopes as a probe of weathering processes: Orinoco River. *Earth and Planetary Science Letters* 194:189–199, http://dx.doi.org/10.1016/S0012-821X(01)00523-4.

Huh, Y., L.H. Chan, L. Zhang, and J.M. Edmond. 1998. Lithium and its isotopes in major world rivers: Implications for weathering and the oceanic budget. *Geochimica Cosmochimica Acta* 62:2,039–2,051, http://dx.doi.org/10.1016/S0016-7037(98)00126-4.

Kent, D.V., and G. Muttoni. 2008. Equatorial convergence of India and early Cenozoic climate trends. *Proceedings of the National Academy of Sciences of the United States of America* 105:16,065–16,070, http://dx.doi.org/10.1073/pnas.0805382105.

Kisakurek, B., R.H. James, and N.B.W. Harris. 2005. Li and δ^7Li in Himalayan rivers: Proxies for silicate weathering? *Earth and Planetary Science Letters* 237:387–401, http://dx.doi.org/10.1016/j.epsl.2005.07.019.

Komar, N., R.E. Zeebe, and G.R. Dickens. 2013. Understanding long-term carbon cycle trends: The late Paleocene through the early Eocene. *Paleoceanography* 28, http://dx.doi.org/10.1002/palo.20060.

Kurtz, A.C., L.R. Kump, M.A. Arthur, J.C. Zachos, and A. Paytan. 2003. Early Cenozoic decoupling of the global carbon and sulfur cycles. *Paleoceanography* 18, 1090, http://dx.doi.org/10.1029/2003PA000908.

Lefebvre, V., Y. Donnadieu, Y. Gdderis, F. Fluteau, and L. Hubert-Theou. 2013. Was the Antarctic glaciation delayed by a high degassing rate during the early Cenozoic? *Earth and Planetary Science Letters* 371–372:203–211, http://dx.doi.org/10.1016/j.epsl.2013.03.049.

Li, G., and H. Elderfield. 2013. Evolution of carbon cycle over the past 100 million years. *Geochimica Cosmochimica Acta* 103:11–25, http://dx.doi.org/10.1016/j.gca.2012.10.014.

Li, G., and J. West. 2014. Evolution of Cenozoic seawater lithium isotopes: Coupling of global denudation regime and shifting seawater sinks. *Earth and Planetary Science Letters* 401:284–293, http://dx.doi.org/10.1016/j.epsl.2014.06.011.

Mackenzie, F.T., and R.M. Garrels. 1966. Chemical mass balance between rivers and oceans. *American Journal of Science* 264:507–525, http://dx.doi.org/10.2475/ajs.264.7.507.

Mackin, J.E. 1986. Control of dissolved Al distribution in marine sediments by clay reconstitution reactions: Experimental evidence leading to a unified theory. *Geochimica et Cosmochimica Acta* 50:207–214, http://dx.doi.org/10.1016/0016-7037(86)90170-5.

Mackin, J.E., and R.C. Aller. 1989. The nearshore marine and estuarine chemistry of dissolved Aluminium and rapid authigenic mineral precipitation. *Reviews in Aquatic Science* 1:537–554.

Martin, E.E., and J.D. Macdougall. 1991. Seawater Sr isotopes at the Cretaceous/Tertiary boundary. *Earth and Planetary Science Letters* 104:166–180, http://dx.doi.org/10.1016/0012-821X(91)90202-S.

Martin, E.E., and H.D. Scher. 2004. Preservation of seawater Sr and Nd isotopes in fossil fish teeth: Bad news and good news. *Earth and Planetary Science Letters* 220:25–39, http://dx.doi.org/10.1016/S0012-821X(04)00030-5.

Martin, E.E., N.J. Shackleton, J.C. Zachos, and B.P. Flower. 1999. Orbitally-tuned Sr isotope chemostratigraphy for the late middle to late Miocene. *Paleoceanography* 14:74–83, http://dx.doi.org/10.1029/1998PA900008.

Mead, G.A., and D.A. Hodell. 1995. Controls on the $^{87}Sr/^{86}Sr$ composition of seawater from the middle Eocene to Oligocene: Hole 689B, Maud Rise, Antarctica. *Paleoceanography* 10:327–327, http://dx.doi.org/10.1029/94PA03069.

Michalopoulos, P., and R.C. Aller. 1995. Rapid clay mineral formation in Amazon delta sediments: Reverse weathering and oceanic elemental cycles. *Science* 270:614–616, http://dx.doi.org/10.1126/science.270.5236.614.

Michalopoulos, P., and R.C. Aller. 2004. Early diagenesis of biogenic silica in the Amazon delta: Alteration, authigenic clay formation, and storage. *Geochimica Cosmochimica Acta* 68:1,061–1,085, http://dx.doi.org/10.1016/j.gca.2003.07.018.

Michalopoulos, P., R.C. Aller, and R.J. Reeder. 2000. Conversion of diatoms to clays during early diagenesis in tropical continental shelf muds. *Geology* 28:1,095–1,098, http://dx.doi.org/10.1130/0091-7613(2000)28<1095:CODTCD>2.0.CO;2.

Miller, K.G., M.D. Feigenson, J.D. Wright, and B.M. Clement. 1991. Miocene isotope reference section, Deep Sea Drilling Project Site 608: An evaluation of isotope and biostratigraphic resolution. *Paleoceanography* 6:33–52, http://dx.doi.org/10.1029/90PA01941.

Millot, R., N. Vigier, and J. Gaillardet. 2010. Behaviour of lithium and its isotopes during weathering in the Mackenzie Basin, Canada. *Geochimica Cosmochimica Acta* 74:3,897–3,912, http://dx.doi.org/10.1016/j.gca.2010.04.025.

Misra, S., and P.N. Froelich. 2012. Lithium isotope history of Cenozoic seawater: Changes in silicate weathering and reverse weathering. *Science* 335:818–823, http://dx.doi.org/10.1126/science.1214697.

Molnar, P. 2004. Late Cenozoic increase in accumulation rates of terrestrial sediment. *Annual Reviews of Earth and Planetary Sciences* 32:67–89, http://dx.doi.org/10.1146/annurev.earth.32.091003.143456.

Pälike, H., M.W. Lyle, H. Nishi, I. Raffi, A. Ridgewell, K. Gamage, A. Klaus, G. Acton, L. Anderson, J. Backman, and others. 2012. A Cenozoic record of the equatorial Pacific carbonate compensation depth. *Nature* 488:609–614, http://dx.doi.org/10.1038/nature11360.

Palmer, M.R., and J.M. Edmond. 1989. The strontium isotope budget of the modern ocean. *Earth and Planetary Science Letters* 92:11–26, http://dx.doi.org/10.1016/0012-821X(89)90017-4.

Palmer, M.R., and J.M. Edmond. 1992. Controls over the strontium isotope composition of river water. *Geochimica Cosmochimica Acta* 56:2,099–2,111, http://dx.doi.org/10.1016/0016-7037(92)90332-D.

Peizhen, Z., P. Molnar, and W.R. Dowes. 2001. Increased sedimentation rates and grain sizes 2–4 Myr ago due to the influence of climate change on erosion rates. *Nature* 410:891–897, http://dx.doi.org/10.1038/35073504.

Pogge von Strandmann, P.A.E., K.W. Burton, R.H. James, P. van Calsteren, and S.R. Gíslason. 2006. Riverine behaviour of uranium and lithium isotopes in an actively glaciated basaltic terrain. *Earth and Planetary Science Letters* 251:134–147, http://dx.doi.org/10.1016/j.epsl.2006.09.001.

Pogge von Strandmann, P.A.E., R.H. James, P. van Calsteren, and S.R. Gíslason. 2008. Lithium, magnesium and uranium isotope behaviour in the estuarine environment of basaltic islands. *Earth and Planetary Science Letters* 274:462–471, http://dx.doi.org/10.1016/j.epsl.2008.07.041.

Rausch, S., F. Bohm, W. Back, A. Kluget, and A. Eisenhauer. 2013. Calcium carbonate veins in ocean crust record a three-fold increase of seawater Mg/Ca in the past 30 million years. *Earth and Planetary Science Letters* 362:215–224, http://dx.doi.org/10.1016/j.epsl.2012.12.005.

Raymo, M.E. 1991. Geochemical evidence supporting T.C. Chamberlin's theory of glaciation. *Geology* 19:344–347, http://dx.doi.org/10.1130/0091-7613(1991)019<0344:GESTCC>2.3.CO;2.

Raymo, M.E., and W.F. Ruddiman. 1992. Tectonic forcing of late Cenozoic climate. *Nature* 359:117–122, http://dx.doi.org/10.1038/359117a0.

Raymo, M.E., W.F. Ruddiman, and P.N. Froelich. 1988. Influence of late Cenozoic mountain building on ocean geochemical cycles. *Geology* 16:649–653, http://dx.doi.org/10.1130/0091-7613(1988)016<0649:IOLCMB>2.3.CO;2.

Reagan, M.K., W.C. McClelland, G. Girard, K.R. Goff, D.W. Peate, Y. Ohara, and R.J. Stern. 2013. The geology of the southern Mariana fore-arc crust: Implications for the scale of Eocene volcanism in the western Pacific. *Earth and Planetary Science Letters* 380:41–51, http://dx.doi.org/10.1016/j.epsl.2013.08.013.

Rowley, D.B. 2002. Rate of plate creation and destruction: 180 Ma to present. *Geological Society of America Bulletin* 114:927–933, http://dx.doi.org/10.1130/0016-7606(2002)114<0927:ROPCAD>2.0.CO;2.

Ruddiman, W.F., M.E. Raymo, W.L. Prell, and J.E. Kutzback. 1997. The uplift-climate connections: A synthesis. Pp. 363–397 in *Tectonic Uplift and Climate Change*. W.F. Ruddiman, ed., Plenum, New York.

Sayles, F.L. 1979. The composition and diagenesis of interstitial solutions: Part I. Fluxes across the seawater-sediment interface in the Atlantic Ocean. *Geochimica et Cosmochimica Acta* 43:527–545, http://dx.doi.org/10.1016/0016-7037(79)90163-7.

Sayles, F.L. 1981. The composition and diagenesis of interstitial solutions: Part II. Fluxes and diagenesis at the water-sediment interface in the high latitude North and South Atlantic. *Geochimica Cosmochimica Acta* 45:1,061–1,086, http://dx.doi.org/10.1016/0016-7037(81)90132-0.

Sluijs, A., S. Schouten, M. Pagani, M. Woltering, H. Brinkhuis, J.S. Sinninghe Damste, G.R. Dickens, M. Huber, G.-J. Reichart, R. Stein, and others. 2006. Subtropical Arctic Ocean temperatures during the Paleocene/Eocene thermal maximum. *Nature* 441:610–613, http://dx.doi.org/10.1038/nature04668.

Sluijs, A., R.E. Zeebe, P.K. Bijl, and S.W. Bohaty. 2013. A middle Eocene carbon cycle conundrum. *Nature Geoscience* 6:429–434, http://dx.doi.org/10.1038/ngeo1807.

Stallard, R.F., and J.M. Edmond. 1981. Geochemistry of the Amazon: Part 1. Precipitation chemistry and the marine contribution to the dissolved load at the time of peak discharge. *Journal of Geophysical Research* 86:9,844–9,858, http://dx.doi.org/10.1029/JC086iC10p09844.

Stallard, R.F., and J.M. Edmond. 1983. Geochemistry of the Amazon: Part 2. The influence of geology and weathering environment on the dissolved load. *Journal of Geophysical Research* 88:9,671–9,688, http://dx.doi.org/10.1029/JC088iC14p09671.

Stallard, R.F., and J.M. Edmond. 1987. Geochemistry of the Amazon: Part 3. Weathering chemistry and limits to dissolved inputs. *Journal of Geophysical Research* 92:8,293–8,302, http://dx.doi.org/10.1029/JC092iC08p08293.

Stoffyn-Egli, P., and F.T. Mackenzie. 1984. Mass balance of dissolved lithium in the oceans. *Geochimica Cosmochimica Acta* 48:859–872, http://dx.doi.org/10.1016/0016-7037(84)90107-8.

Svensen, H., S. Planke, A. Maltke-Sorenssen, B. Jamtveit, T.R. Miltebest, and S.S. Eiden. 2004. Release of methane from a volcanic basin as a mechanism for initial Eocene global warming. *Nature* 429:542–545, http://dx.doi.org/10.1038/nature02566.

Urey, H.C., and S.A. Korff. 1952. The planets: Their origin and development. *Physics Today* 5:12.

Vigier, N., A. Decarreau, R. Millot, J. Carignan, S. Petit, and C. France-Lanord. 2006. Quantifying the isotopic fractionation of lithium during clay formation at various temperatures. *Geochimica Cosmochimica Acta* 70:A673, http://dx.doi.org/10.1016/j.gca.2006.06.1258.

Vigier, N., A. Decarreau, R. Millot, J. Carignan, S. Petit, and C. France-Lanord. 2008. Quantifying Li isotope fractionation during smectite formation and implications for the Li cycle. *Geochimica Cosmochimica Acta* 72:780–792, http://dx.doi.org/10.1016/j.gca.2007.11.011.

Vigier, N., S.R. Gislason, K.W. Burton, R. Millot, and F. Mokadem. 2009. The relationship between riverine lithium isotope composition and silicate weathering rates in Iceland. *Earth and Planetary Science Letters* 287:434–441, http://dx.doi.org/10.1016/j.epsl.2009.08.026.

Walker, J.C.G., P.B. Hays, and J.F. Kasting. 1981. A negative feedback mechanism for the long-term stabilization of Earth's surface temperature. *Journal of Geophysical Research* 86:9,776–9,782, http://dx.doi.org/10.1029/JC086iC10p09776.

West, A.J. 2012. Thickness of the chemical weathering zone and implications for erosional and climatic drivers of weathering and for carbon-cycle feedbacks. *Geology* 40:811–814.

West, A.J., A. Galy, and M. Bickle. 2005. Tectonic and climatic controls on silicate weathering. *Earth and Planetary Science Letters* 235:211–228, http://dx.doi.org/10.1016/j.epsl.2005.03.020.

Wimpenny, J., R.H. James, K.W. Burton, A. Gannou, F. Mokadem, and S.R. Gíslason. 2010. Glacial effects on weathering processes: New insights from the elemental and lithium isotopic composition of West Greenland rivers. *Earth and Planetary Science Letter* 290:427–437, http://dx.doi.org/10.1016/j.epsl.2009.12.042.

Zachos, J.C., G.R. Dickens, and R.E. Zeebe. 2008. An early Cenozoic perspective on greenhouse warming and carbon-cycle dynamics. *Nature* 451:279–283, http://dx.doi.org/10.1038/nature06588.

Zachos, J.C., M. Pagani, L. Sloan, E. Thomas, and K. Billups. 2001. Trends, rhythms, and aberrations in global climate 65 Ma to present. *Science* 292:686, http://dx.doi.org/10.1126/science.1059412.

Zachos, J.C., U. Rohl, S.A. Schellenberg, A. Sluijs, D.A. Hodell, D.C. Kelly, E. Thomas, M. Nicolo, I. Raffi, L.J. Lourens, and others. 2005. Rapid acidification of the ocean during the Paleocene-Eocene Thermal Maximum. *Science* 308:1,611–1,615, http://dx.doi.org/10.1126/science.1109004.

Zeebe, R.E. 2013. What caused the long duration of the Paleocene-Eocene Thermal Maximum? *Paleoceanography* 3:440–452, http://dx.doi.org/10.1002/palo.20039.